https://doi.org/10.26599/FRICT.2026.9441263

Research Article

Enhanced interfacial mechanical properties by micro-nano structures via self-assembly mask etching

Zeyu Wang[1], Yiming Li[2], Xuanhe Zhang[2], Yuan Gao[1], Hua Qin[1]✉, Yuan Ma[2]✉, Jiadao Wang[2]✉

[1]School of Mechanical-Electronic and Vehicle Engineering, Beijing University of Civil Engineering and Architecture, Beijing 102616, China;

[2]Department of Mechanical Engineering, Tsinghua University, Beijing 100084, China;

Zeyu Wang and Yiming Li contributed equally to this work and share first authorship.

✉ Corresponding author. E-mail:qinhua@bucea.edu.cn (Hua Qin); yuanma@tsinghua.edu.cn (Yuan Ma);jdwang@mail.tsinghua.edu.cn(Jiadao Wang)

Received: December 18, 2025; Revised: March 23, 2026; Accepted: May 7, 2026

Abstract: Heterogeneous composite materials are widely used in microelectronic, optoelectronic, and flexible devices, yet their reliability is often limited by insufficient interfacial bonding strength and thermal mismatch–induced failure.Here, a generally applicable interfacial enhancement strategy based on microsphere self-assembly mask etching is proposed, in which ordered micro–nano structure arrays

are constructed on substrate surfaces to simultaneously improve interfacial mechanical properties and thermal stability.By combining periodic microsphere self-assembled masks with dry etching, structurally consistent micro–nano architectures can be rapidly fabricated on both inorganic and polymer substrates without high-temperature processing.Representative systems including Cu/SiO_2, Cu/poly(methyl methacrylate) (PMMA), and indium tin oxide (ITO)/PMMA are systematically investigated using nano-scratch, micro-scratch, pull-off, and thermal shock tests.The results show that the micro–nano structures significantly enhance interfacial bonding by increasing the effective contact area and inducing strong mechanical interlocking.For the Cu/SiO_2 system, nanoscale Cu coatings remain intact without delamination under an 80 mN load, while the critical failure load of microscale coatings increases from 6.53 N to 16.62 N.In the Cu/PMMA system, nano-scratch tests reveal an increase in interfacial failure load from 5.53 mN to 45.05 mN, accompanied by a transition from interfacial delamination to coupled coating damage and substrate structural collapse, and the pull-off bonding strength of microscale coatings is further improved by ~49%.Moreover, the micro–nano structures effectively suppress cracking and wrinkling of ITO coatings on PMMA under thermal shock conditions up to 80 °C.This work provides a simple, low-damage, and broadly applicable route for strengthening heterogeneous interfaces and improving thermal reliability in advanced electronic and flexible systems.

Keywords:heterogeneous composite materials,micro-nano structures,interfacial mechanical properties,interfacial bonding strength,thermal stability

1 Introduction

Heterogeneous composite materials achieve the integration of multiple properties that a single material cannot achieve by organically combining components with different physical, chemical, and mechanical properties at the micro or macro scale. As a result, they exhibit irreplaceable application value in fields such as microelectronic devices, biomedical implants, and high-performance functional coatings[1-8].Numerous studies have shown that the macroscopic service performance of such materials, including overall strength, durability, and long-term functional stability, depends not only on the intrinsic properties of the constituent materials but also, to a large extent, on the structural characteristics and bonding quality of the interface between heterogeneous phases[9-12].

In practical engineering applications, heterogeneous interfaces often have to withstand complex mechanical loads, friction and wear, as well as repeated thermal cycling conditions[13-15].Therefore, the bonding strength of the interface and its stability under high temperature or thermal shock conditions are particularly critical.However, due to significant differences in crystal structure, thermal expansion coefficients, and chemical reactivity between heterogeneous materials, achieving an interface with both high bonding strength and high stability has always been a challenging task[16-20].

In recent years, strategies aimed at enhancing the interfacial mechanical properties of coating/substrate systems by introducing micro-nano structures onto substrate surfaces have attracted widespread attention[20-24].Related studies have demonstrated that appropriate surface structuring can significantly enhance the mechanical stability of heterogeneous interfaces by increasing the effective contact area and introducing mechanical interlocking.For example, Cao et al.[25] demonstrated that depositing SiO_2 particles onto Carbon fiber reinforced polymer matrix surfaces can effectively improve the interfacial bonding strength of coatings, with the enhancement mechanism

mainly attributed to the synergistic increase in surface roughness and surface energy.On the other hand, Yu et al.[26] fabricated regular micro-textures using nanosecond laser processing and achieved a significant improvement in the interfacial bonding strength between ceramic substrates and plasma-sprayed coatings, thereby verifying the effectiveness of controllable microstructures in interfacial reinforcement.Nevertheless, the unavoidable heat-affected zones, the introduction of residual stresses, and the relatively high equipment and processing costs associated with laser processing constrain its applicability for heat-sensitive substrates or large-area fabrication scenarios.

Overall, existing studies have demonstrated the beneficial effects of micro-nano structures on improving the interfacial mechanical properties of heterogeneous interfaces.Nevertheless, notable limitations remain with respect to the precise control of structural dimensions, the simplicity of fabrication processes, and the general applicability to different substrate materials.To overcome these limitations, a surface micro-nano structure fabrication approach based on microsphere mask etching is proposed in this work.Ordered arrays formed by microsphere self-assembly are used as etching masks and combined with dry etching to rapidly generate micro-nano structures, while eliminating the thermal damage commonly associated with laser-based processing.In addition, this approach exhibits low dependence on the chemical nature of substrate materials, enabling the rapid fabrication of structurally consistent micro-nano structure arrays on a wide range of substrates, including inorganic materials and polymers.Representative engineering materials[27-29], including SiO_2, poly(methyl methacrylate) (PMMA), Cu, and indium tin oxide (ITO), were selected as model substrates, and multi-scale, multi-perspective mechanical and reliability testing methods[20,30,31] were employed to quantitatively investigate the enhancement of interfacial bonding strength and thermal stability induced by microcones under coatings with different thicknesses.This strategy provides a practically

viable interfacial regulation approach for the systematic enhancement of the interfacial mechanical properties of coating/substrate systems.

2 Methods

2.1 Sample Preparation

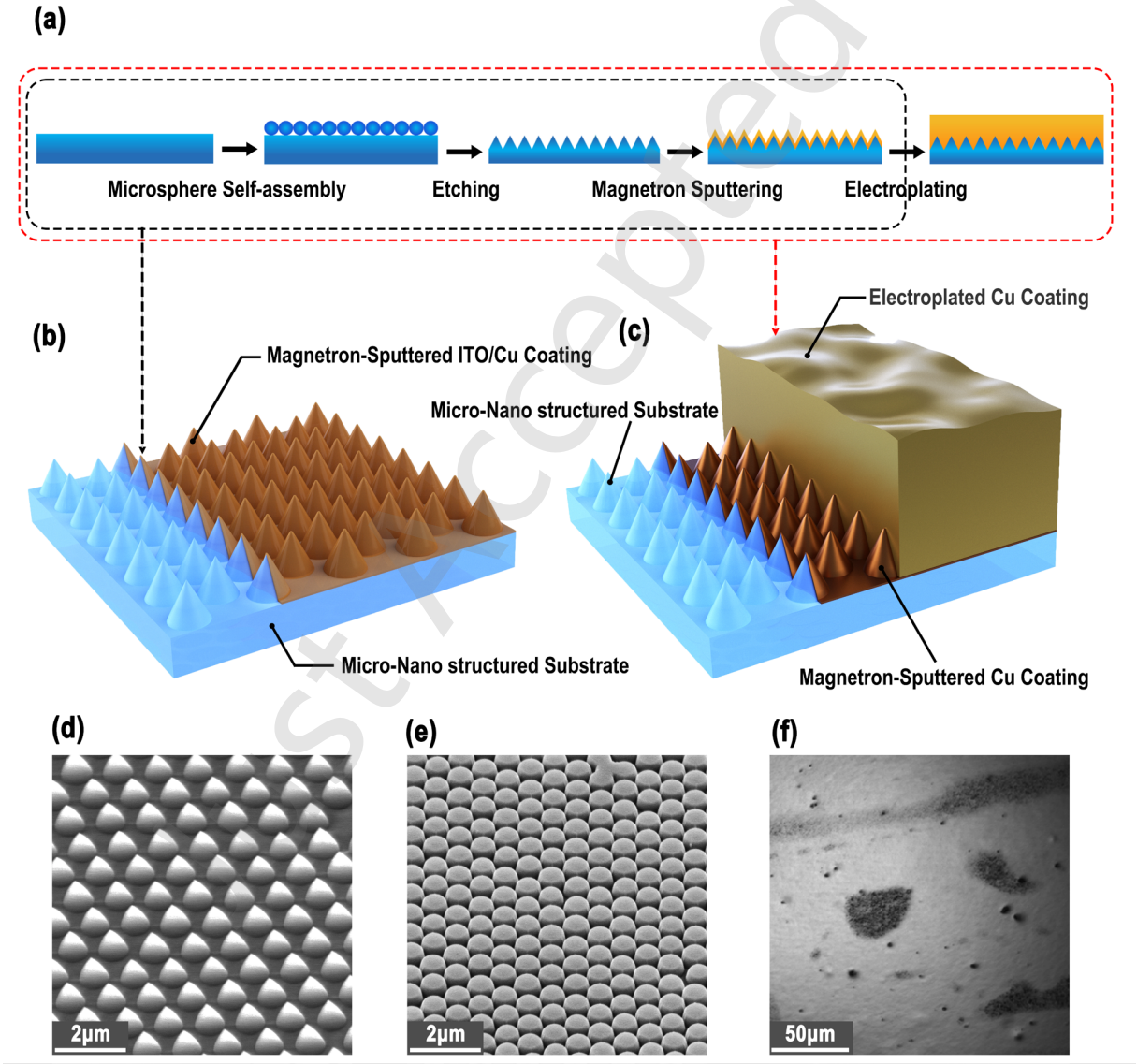

Fig. 1 Process flow and structural characterization:(a) schematic of the fabrication process.(b) schematic diagram of the nanoscale-coated micro-nano structured substrate.(c) schematic diagram of

the microscale-coated micro-nano structured substrate.(d) characterization of the micro-nano structures. (e) characterization of the nanoscale-coated sample.(f) characterization of the microscale-coated sample.

In this study, we selected SiO_2, a typical ceramic material, and PMMA, a representative organic material, as substrate materials, while Cu and the metal oxide ITO were chosen as representative coating materials. Their key mechanical properties are provided in Table. S1. Coating thicknesses of 240 nm and 13 μm were used to represent nanoscale and microscale coatings, respectively. To ensure the consistency of material properties among coatings with the same thickness, indentation tests were conducted, and the results are presented in Fig. S1.The fabrication process of the micro-nano structured heterogeneous composite samples is shown in Fig. 1(a). Specifically, a monolayer of nanospheres was first self-assembled on the substrate surface to serve as a mask, with 900 nm diameter SiO_2 microspheres used for SiO_2 substrates and 900 nm diameter polystyrene (PS) microspheres used for PMMA substrates. Inductively coupled plasma (ICP) dry etching was then employed to etch the substrate. For SiO_2 substrates, the etching parameters were as follows: C_4F_8/Ar gas flow rate of 20/80 sccm, ICP power of 500 W, RF power of 200 W and etching time of 90 s. For PMMA substrates, O_2 plasma etching was employed with an O_2 flow rate of 40 sccm, RF power of 200 W and etching time of 90 s. During the etching process, the microspheres used as the mask gradually decreased in size and eventually disappeared as the etching time increased, which caused the exposed area of the substrate to expand continuously. This process resulted in the formation of micro-nano structures on the substrate, as characterized in Fig. 1(d). Figures 1(b) and 1(e) show the nanoscale coating deposited on the substrate using magnetron sputtering.To further investigate the interfacial structure, focused ion beam (FIB) milling and SEM analysis were performed on the cross-section of the coated sample; the

results are presented in Fig. S2. For microscale coatings, as shown in Figures 1(c) and 1(f), an electroplating process was used to further thicken the nanoscale Cu seed layer to the microscale level.

2.2 Interfacial Bonding Strength Testing

2.2.1 Scratch Test

The interfacial bonding strength of the nanoscale coating was measured using a nano-scratch tester (Nano-Hardness, Anton Paar). The test employed a 10 μm diameter spherical indenter under a linearly increasing normal force, with the loading force range selected according to different samples, a scratch length of 100 μm, and a data acquisition rate of 40 Hz. The scratch velocity was maintained at 1.67 μm/s throughout the test. Additionally, the microstructure of the scratch was examined using a scanning electron microscope (HITACHI SU8220, Hitachi). Elemental analysis of the scratch surface was performed using an X-ray energy spectrometer (QUANTAX FlatQUAD, Bruker) equipped with the scanning electron microscope.

The interfacial bonding strength of the microscale coating on the SiO_2 substrate was measured using a micro-scratch tester (RTEC MFT-2000A, Rtec Instruments).The test employed a 200 μm diameter spherical indenter under a linearly increasing normal force, with the loading force range selected according to different samples, a scratch length of 2 mm, and a data acquisition rate of 100 Hz. The scratch velocity was maintained at 33.3 μm/s. This force range was uniformly applied for all microscale coating samples. The instrument integrates a confocal 3D profilometer, which was used to characterize the scratch morphology and perform three-dimensional modeling after the scratch test.

2.2.2 Pull-off Test

The interfacial bonding strength of the microscale coating on the PMMA substrate was tested using a peel-off method. A tensile testing machine (HN-603, ZGDR) was employed, with a 10 mm diameter

acrylic cylinder and UV adhesive used to bond the coating to the tensile testing instrument. The force at which the coating delaminated was obtained from the vertical displacement-force curve provided by the instrument. The delamination area was measured using ImageJ software to quantify the bonding strength between the microscale Cu coating and PMMA substrate.

2.3 Thermal Shock Test

The thermal stability of the samples was tested using a thermal shock test. The samples were heated using a desktop curing oven (HP10, LEBO), and the actual temperature of the samples was measured with a thermal imaging thermometer (P09, HIKMICRO) to ensure that the surface temperature reached the preset value. After heating to the preset temperature, a 10-minute holding time was maintained, and the samples were then allowed to cool to 20°C in air. The samples were characterized using a metallographic microscope (UM103i, UOP) after the test.

The samples were heated from 20 °C to the target temperature at a heating rate of approximately 5 °C/min, held at the target temperature for 10 minutes to ensure uniform temperature distribution, and then cooled naturally in ambient air to room temperature.

3 Results and Discussion

3.1 Theoretical Background

3.1.1 Mechanisms of Bonding Strength Enhancement

For a planar substrate interface, the bonding force between the coating and the substrate mainly originates from adhesive interactions between interfacial atoms or molecules. The magnitude of this force can be approximately expressed as the product of the interfacial bonding strength and the apparent contact area[32]:

$$F_{planar}=\sigma \cdot A_{planar} \quad (1)$$

Where

σ is the interfacial bonding strength,

A_{planar} is the apparent area of the planar substrate.

When micro-nano structures are introduced onto the substrate surface, the interfacial bonding mechanism changes significantly.On the one hand, the micro-nano structures markedly increase the effective contact area of the interface, on the other hand, the coating can undergo plastic flow under external loading and penetrate into the micro-nano scale gaps, thereby introducing a pronounced mechanical interlocking effect.Accordingly, the total bonding force of the micro-nano structured interface can be expressed as:

$$F_{micro-nano}=\sigma \cdot A_{eff}+F_{mech} \quad (2)$$

Where:

A_{eff} is the effective contact area, including the contribution from the sidewalls of the micro-nano structures,

F_{mech} represents the mechanical interlocking force introduced by the micro-nano structures.

To quantitatively evaluate the contribution of the increased effective contact area, a geometric model is established based on the actual dimensions of the micro-nano structure arrays. As characterized in Fig. 1(d), the micro-nano structures exhibit an average height of $h\approx0.55$ μm,a base diameter of $d\approx0.8$ μm,and a periodicity of $p\approx0.9$ μm.Assuming an ideal conical geometry, the lateral surface area of a single structure, $A_{structure}$ is calculated as:

$$A_{structure}=\pi \cdot \frac{d}{2} \cdot \sqrt{\left(\frac{d}{2}\right)^2+h^2} \quad (3)$$

Within each periodic unit cell of area p^2, the effective contact area A_{eff} includes both the structure sidewall and the surrounding flat region. Therefore, the surface area enlargement factor λ is expressed

as:

$$\lambda=\frac{A_{eff}}{A_{planar}}=\frac{A_{structure}+(p^2-\pi(\frac{d}{2})^2)}{p^2}\approx 1.43 \quad (4)$$

This calculation indicates that the micro-nano structures enlarge the effective contact area of the substrate surface to approximately 1.43 times that of a planar substrate. Because $A_{eff}>A_{planar}$ and $F_{mech}>0$,the bonding force of the micro-nano structured interface is significantly higher than that of the planar interface. This provides a theoretical basis for the pronounced increase in the critical failure load observed in subsequent experiments.

3.1.2 Mechanisms of Enhanced Thermal Stability

According to classical thermoelastic theory, temperature variations generate thermal mismatch stress ($\sigma_{thermal}$) at the interface due to the difference in thermal expansion coefficients between the coating and the substrate, which can be expressed as:

$$\sigma_{thermal}=\frac{E}{1-\nu}\cdot\Delta\alpha\cdot\Delta T \quad (5)$$

Where:

E is the Young's modulus of the coating,

ν is the Poisson's ratio of the coating,

$\Delta\alpha$ is the difference in thermal expansion coefficients between the substrate and the coating,

ΔT is the temperature change.

According to Griffith's crack theory, cracking occurs in the coating when the thermal mismatch stress $\sigma_{thermal}$ exceeds the fracture strength σ_f, where σ_f can be expressed as:

$$\sigma_f=\sqrt{\frac{E\cdot G_c}{\pi\cdot a}} \quad (6)$$

Where:

G_c is the fracture energy,

a is the initial crack length.

On a planar interface, cracks can propagate linearly along the interface with a short propagation path, requiring relatively low energy.In contrast, the micro-nano structures force any propagating crack to deviate along the sidewalls of the micro-nano structures, thereby extending the crack propagation path. The increased path length implies that more energy is required to create new fracture surfaces.As a result, the fracture energy of the micro-nano structured interface is much higher than that of the planar interface. According to Eq. (6), the corresponding fracture strength is therefore substantially increased, making the interface less susceptible to microcrack damage induced by thermal mismatch stress.

3.2 Effect of Micro-Nano Structure on the Bonding Strength of Cu/SiO_2 Composites

3.2.1 Bonding Strength of Nanoscale Cu Coating on SiO_2 Substrate

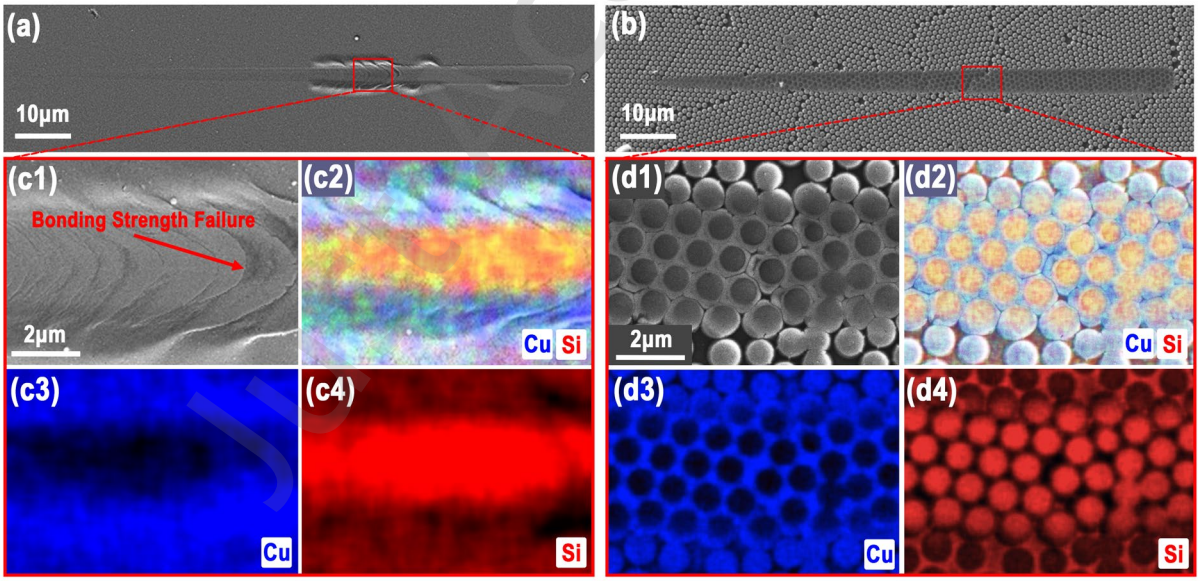

Fig. 2 Nano-scratch tests on Cu/SiO_2 heterogeneous composites:(a) Cu/planar SiO_2(b) Cu/micro-nano structured SiO_2.(c) Scratch characterization of Cu/planar SiO_2.(d) Scratch characterization of Cu / micro-nano structured SiO_2.

There are typically five methods to determine the critical point of coating failure: the abrupt

change in scratch depth, the sudden change in friction force, the sudden change in acoustic emission energy, the abrupt change in friction coefficient, and the observation of the initial damage point of the scratch through a microscope[33-35]. Considering the film thickness and coating material, a 10 μm diameter spherical indenter is used for the scratch test.As shown in Fig. S3, for the Nano-scratch tests, it is not possible to determine the failure point of the coating based solely on the scratch data. Therefore, scanning electron microscopy (SEM) characterization is used as the criterion for evaluating the failure and a quantitative criterion for determining coating failure based on SEM observations has been established: coating failure is considered to have occurred when the continuous length of failure phenomena (such as cracking, delamination, or wrinkling) along the scratch track exceeds 80% of the indenter diameter. Representative SEM images illustrating the application of this criterion for nanoscale coatings have been included in Fig. S4. The subsequent Cu/PMMA Nano-scratch tests are conducted in the same manner.

Figures 2(a) and 2(c) show the results of the Cu coating on planar SiO_2 substrate scratch test. The surface distribution characterization results indicate that at a normal force of 25.09 mN, the SiO_2 substrate is exposed. At this point, the Cu coating in the scratch undergoes damage and plastic deformation due to the normal and tangential stresses applied by the spherical indenter. Additionally, the Cu coating accumulates a large amount of elastic strain energy in the stressed region, which then triggers an instability phenomenon. This phenomenon is manifested as wrinkles in the scratch and delamination of the Cu coating from the substrate on both sides, resulting in protrusions.

As shown in Figures 2(b) and 2(d), during the Cu coating on micro-nano structured SiO_2 substrate scratch test, the Cu coating exhibits phenomena distinct from those observed in the scratch test on planar substrates. At the initial stage of the scratch, the Cu at the top of the micro-nano structures is

pushed into the gaps by the spherical indenter. As the normal force increases, even under a loading force of 80 mN, no delamination of the Cu coating is observed. Instead, more Cu is observed to be squeezed by the indenter and embedded into the gaps between the micro-nano structures . This embedding phenomenon is direct evidence of the strong mechanical interlocking effect provided by the micro-nano structure.

3.2.2 Bonding Strength of Microscale Cu Coating on SiO_2 Substrate

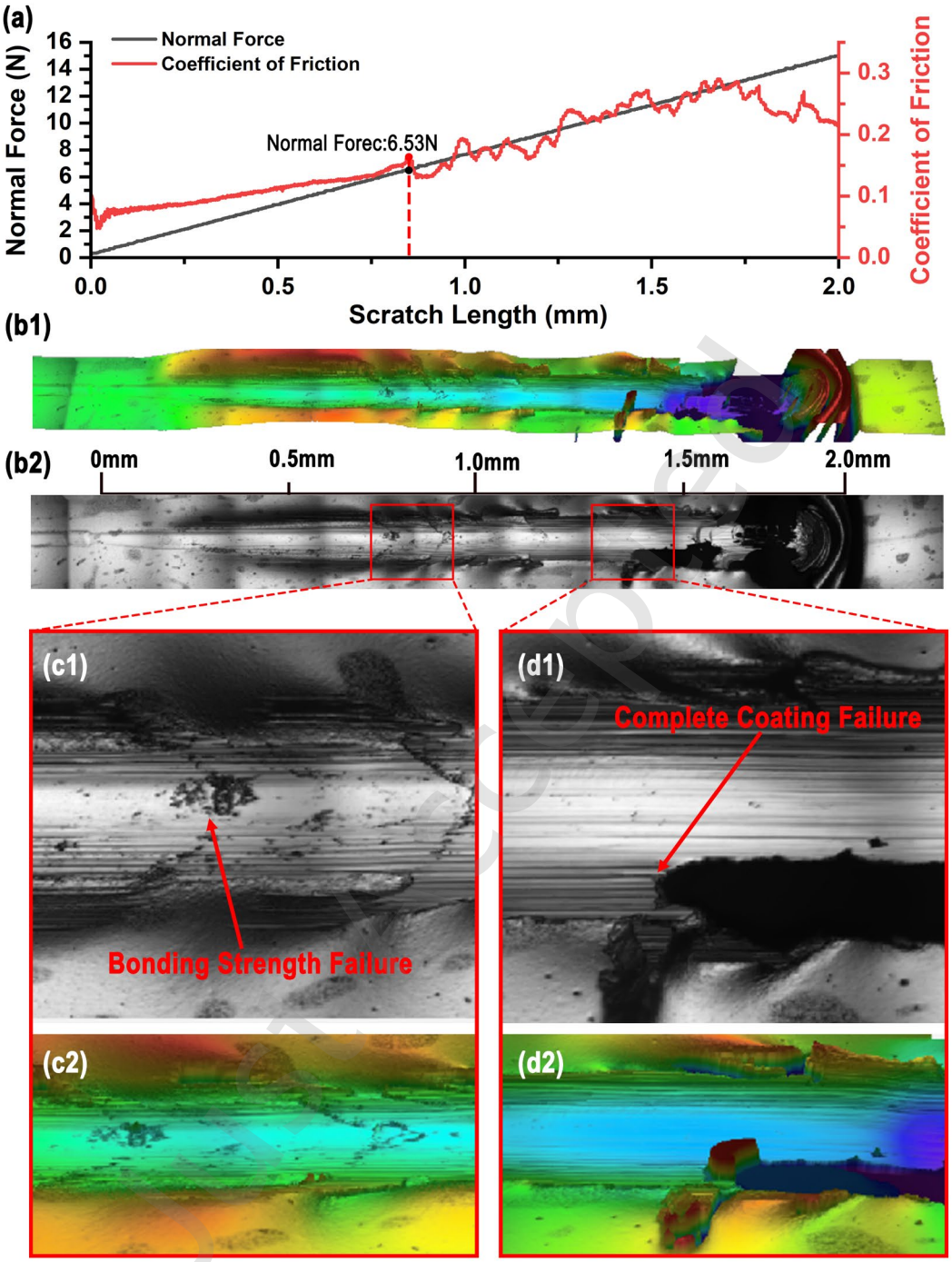

Fig. 3 Micro-scratch tests on Cu/planar SiO_2:(a) Cu/planar SiO_2 scratch test data.(b) Cu/planar SiO_2 scratch characterization.(c) Coating damage characterization.(d) Coating delamination characterization.

A 200 μm diameter spherical indenter is used for the scratch test on microscale Cu coating samples. As shown in Figure 3(a), for the Cu coating on planar SiO_2 substrate samples, as the normal loading

force increases, the friction force shows a nearly linear increase. This linear growth reflects a stable contact and friction mechanism between the indenter and the Cu coating[34]. When the loading force reaches 6.53 N, a jump in the friction force occurs, and arcuate damage appears in the Cu coating in the scratch. This indicates that the bonding strength between the coating and the substrate is insufficient to resist the continuously increasing shear stress[30].After the friction force exhibits a jump, further increases in the applied load lead to intense fluctuations in the friction force, which correspond to the detachment of debris and a transition in the contact material characteristics beneath the indenter[33].

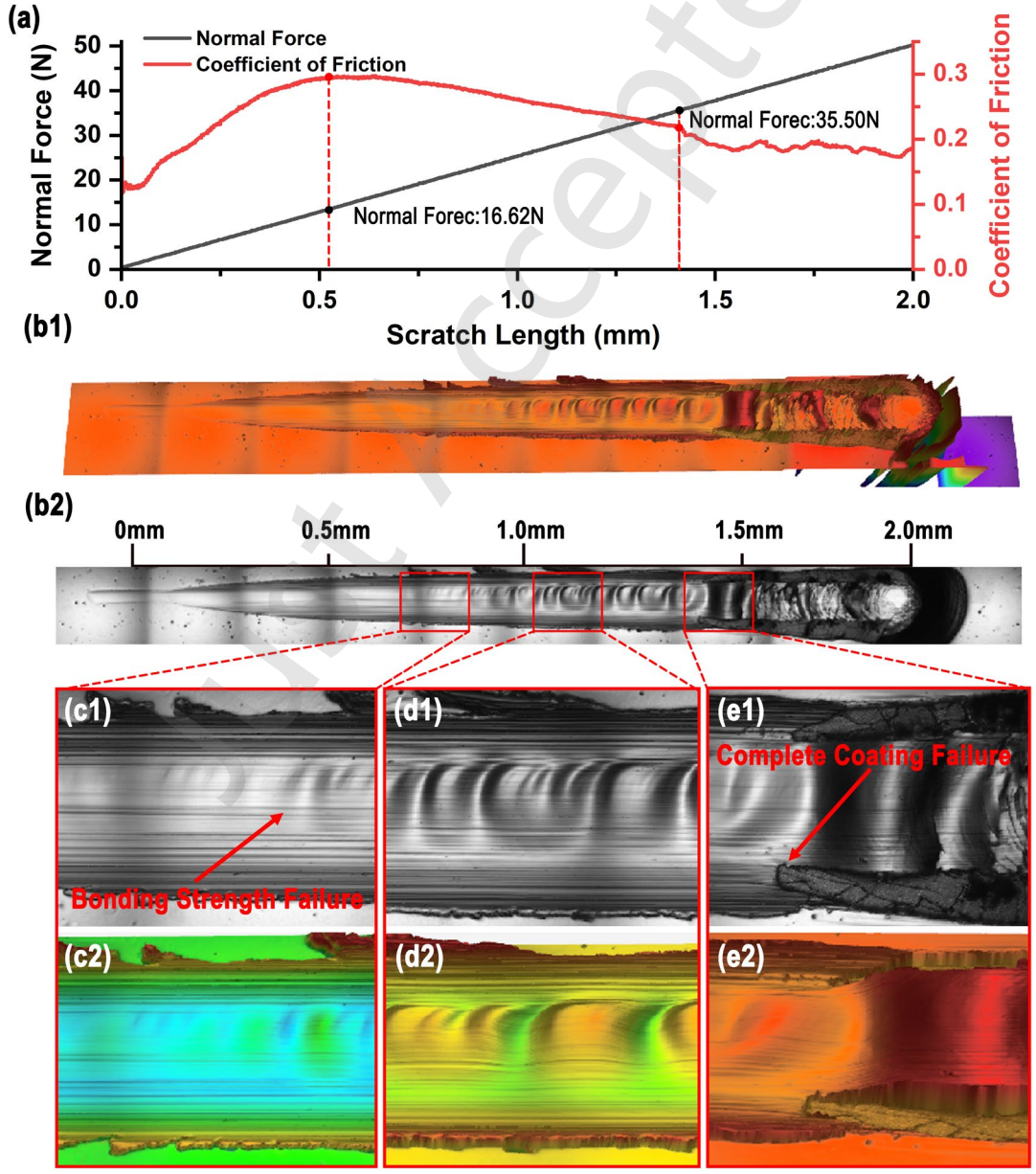

Fig. 4 Micro-scratch tests on Cu/micro-nano structured SiO_2:(a) Cu/micro-nano structured SiO_2 scratch test data.(b) Cu/micro-nano structured SiO_2 scratch characterization.(c) Bonding strength failure characterization.(d) Coating instability characterization.(e) Coating delamination characterization.

As shown in Figures 4(a) and 4(b), the Cu coating on nanocoMicro-scratch testsne-structured SiO_2 substrate scratch test exhibits three stages of friction force variation. In the first stage, as the normal force increases, the friction force gradually increases, reaching its peak at a loading force of 16.62 N. As shown in Figure 4(c), at this point, bonding strength failure occurs, and the Cu coating begins to separate from the substrate. Additionally, the Cu coating undergoes plastic deformation under the normal and tangential forces, resulting in protrusions. In the second stage, as the normal force further increases, the friction force begins to decrease linearly with the normal force, as shown in Figures 4(a) and 4(d). During this stage, the height of the protrusions on the Cu coating surface further increases, but no intense fluctuation in friction force occurs due to bonding strength failure. This may be because the Cu coating undergoes plastic deformation between the micro-nano structures , is squeezed by the indenter, and embedded into the gaps between the micro-nano structures . This plastic flow of Cu and the mechanical interlocking effect formed between the Cu coating and the micro-nano structured substrate change the effective contact area and friction mechanism between the indenter and the coating. In the third stage, the friction force jumps at a loading force of 35.5 N, as shown in Figure 4(e), where the Cu coating on both sides of the scratch experiences damage and delamination, exposing the micro-nano substrate. Subsequently, the friction force becomes chaotic as the loading force increases. This indicates that when the loading force is sufficient to overcome the mechanical interlocking provided by the micro-nano structure, the coating delaminates. However, due to the

presence of the micro-nano structure, this failure is not simple delamination but is accompanied by damage to the Cu coating itself and partial exposure of the micro-nano structure. The subsequent friction force disruption also reflects the unstable contact between the indenter and the complex failure surface.

3.3 Effect of Micro-Nano Structure on the Bonding Performance of Cu/PMMA and ITO/PMMA Composites

3.3.1 Bonding Strength of Nanoscale Cu Coating on PMMA Substrate

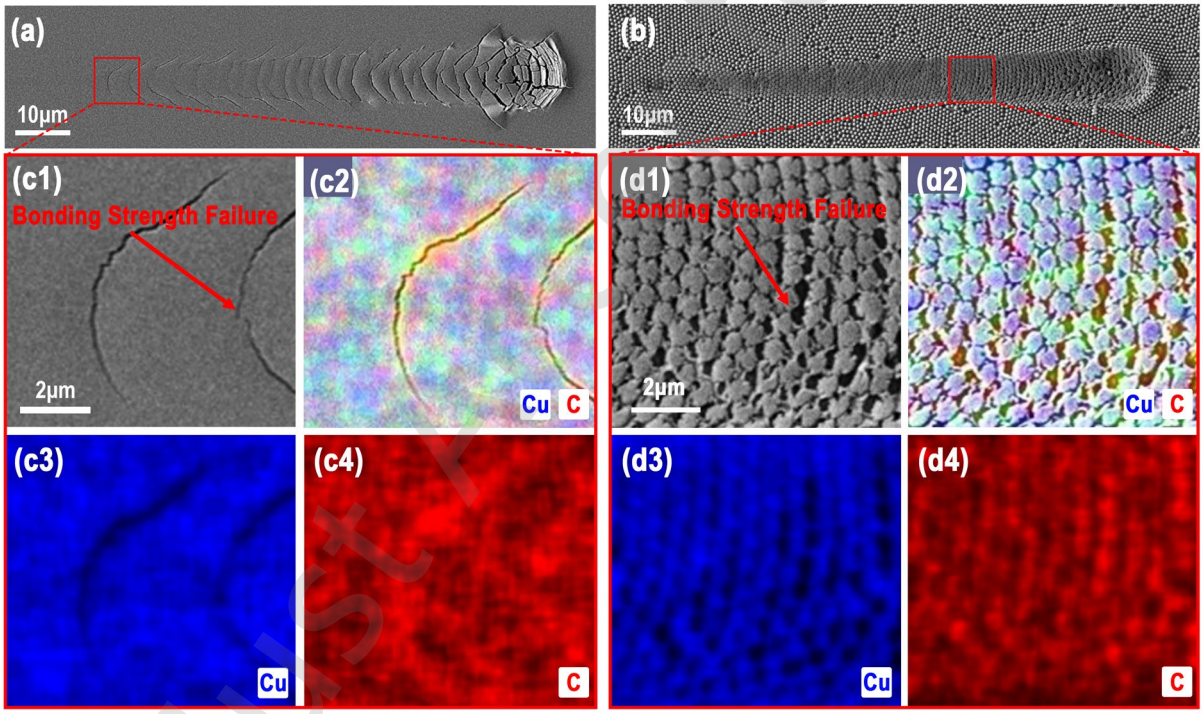

Fig. 5 Nano-scratch tests on Cu/PMMA:(a)Cu/planar PMMA.(b)Cu /micro-nano structured PMMA.(c)Scratch characterization of Cu /planar PMMA.(d) Scratch characterization of Cu / micro-nano structured PMMA.

As shown in Figures 5(a) and 5(c), the results of the Cu coating on planar PMMA substrate scratch

test indicate that at a loading force of 5.53 mN, the Cu coating exhibits arcuate damage, at which point bonding strength failure occurs. From the results of the Cu coating on micro-nano structured PMMA substrate scratch test shown in Figures 5(b) and 5(d), it can be seen that at a loading force of 45.05 mN, the micro-nano structures are crushed. The surface distribution results show that the Cu coating experiences damage, and bonding strength failure occurs at this point.

In comparison to the experimental phenomena observed in Section 3.2.1 for the Cu/SiO_2 heterogeneous composites, the bonding strength improvement effect of the micro-nano structure on Cu/PMMA heterogeneous composites is slightly lower. This is because the Young's modulus and hardness of the PMMA substrate are much lower than those of SiO_2, and its micro-nano structure is more prone to plastic deformation or crushing under high loads. As a result, on the micro-nano structured PMMA substrate, the Cu coating under higher loading forces does not simply delaminate or fully embed, but both phenomena occur simultaneously. From Figures 5(b) and 5(d), it can be observed that the failure mode shifts from interface delamination to damage of the coating itself and plastic deformation of the substrate structure. The mechanical properties of the substrate material limit the mechanical interlocking effect induced by the micro-nano structure.

These observations suggest that for soft substrates such as PMMA, the micro-nano structure design needs to be optimized to enhance its mechanical stability, for instance by reducing the aspect ratio to prevent structural collapse or increasing the structural density to better distribute contact stress, thereby preserving structural integrity while maximizing the mechanical interlocking effect and further improving the interfacial bonding strength.

3.2.2 Bonding Strength of Microscale Cu Coating on PMMA Substrate

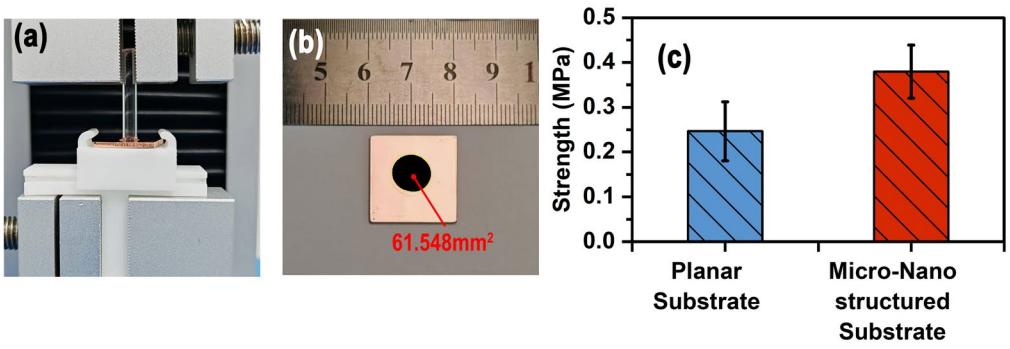

Fig. 6 Pull-off tests on Cu/PMMA:(a) Pull-off test.(b) Pull-off area characterization.(c) Comparison of bonding strength between Cu/PMMA on planar and micro-nano structured substrates.

In the experiment of Section 3.3.1, the crushing of PMMA micro-nano structures is observed. This suggests that in traditional scratch tests, the normal force applied may cause the PMMA substrate to deform or even structurally damage before the coating delaminates. If the substrate is damaged before reaching the critical load for coating failure, the true bonding strength between the coating and the substrate cannot be accurately reflected[12,31,36]. Therefore, we design a pull-off test, as shown in Figure 6(a), to measure the bonding strength of the Microscale Cu Coating on PMMA Substrate. In the test, when the pulling force reaches the maximum stress limit the interface can withstand, the interface bonding fails instantaneously, and the Cu coating rapidly detaches from the PMMA substrate. As shown in Figure 6(b), the peel-off area of the Cu coating is measured using ImageJ software, and the bonding strength is calculated from the pull-off force at the moment of Cu coating detachment. We perform five sets of experiments for both planar PMMA substrate samples and micro-nano PMMA substrate samples, and average the results.The specific experimental data can be found in Table. S2. As shown in Figure 6(c), compared to Cu/planar PMMA heterogeneous composites, the bonding strength of Cu/micro-nano structured PMMA heterogeneous composites increases by 49.37 %.

3.3.3 Thermal Stability of Nanoscale ITO Coating on PMMA Substrate

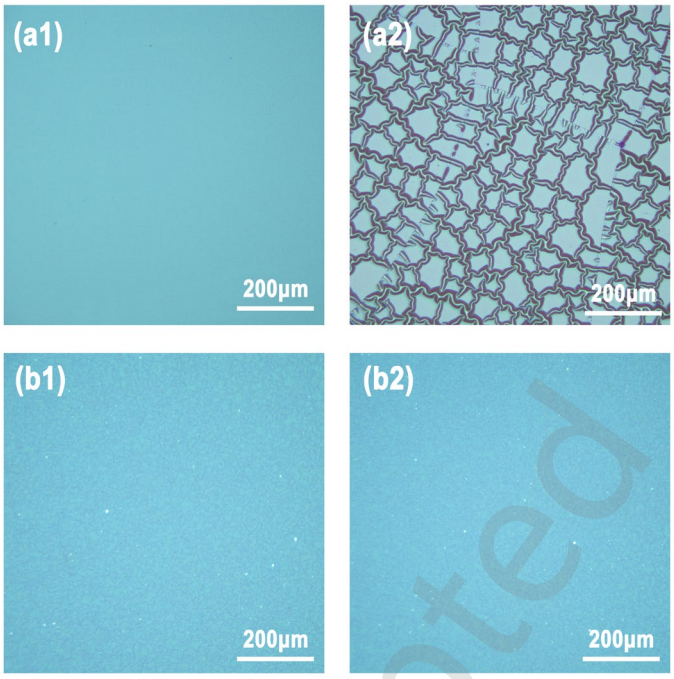

Fig. 7 Thermal shock tests:(a) ITO/planar PMMA 70°C thermal shock test characterization.(b) ITO/micro-nano structured PMMA 70 ℃ thermal shock test characterization.

We select the ITO/PMMA system as a case study to validate the enhancement of thermal stability in heterogeneous composites by micro-nano structures. As shown in Figure 7(a), the ITO/planar PMMA composite exhibits significant cracking and wrinkling under 70 ℃thermal shock conditions. This is primarily due to the significant thermal expansion coefficient mismatch between PMMA and ITO[18]. As a polymer, PMMA has a much higher thermal expansion coefficient than the ITO coating. When the temperature increases, the expansion of the PMMA substrate greatly exceeds that of the ITO coating, causing the ITO layer to experience significant thermal mismatch tensile stress. When the thermal mismatch tensile stress exceeds the fracture strength of ITO, cracking occurs in the ITO coating. During the cooling process, the contraction of PMMA exceeds that of ITO, causing compressive thermal mismatch stress on the ITO. At this point, local instability of the ITO coating occurs, resulting in wrinkling[8,17,37].To enable a more objective comparison, the failure of

ITO/PMMA composites after thermal shock tests was quantified, and the results are presented in Table. S3.

As shown in Figure 7(b), the ITO/micro-nano structured PMMA does not exhibit any significant failure under 70 ℃ thermal shock conditions. This result indicates that the micro-nano structure improves the thermal stability of the heterogeneous composite.We further conduct an 80 °C thermal shock experiment (see Fig. S5) and thermal cycling tests (see Fig. S6) on the ITO/micro-nano structured PMMA to explore the upper limit of thermal stability enhancement by the micro-nano structure. Under the 80 ℃ thermal shock conditions and after 10 thermal cycles, the ITO/micro-nano structured PMMA does not show any significant failure. However, further temperature increases cause the PMMA substrate to transition from the glassy state to the rubbery state, significantly increasing the substrate's thermal expansion coefficient and resulting in deformation. This leads to a change in the failure mode between PMMA and the ITO coating, from thermally stress-driven failure to substrate deformation-driven failure. Therefore, no further high-temperature thermal shock experiments are conducted.

4. Conclusion

This study proposes an interfacial enhancement strategy based on microsphere self-assembly mask etching, in which ordered micro-nano structure arrays are constructed on substrate surfaces to significantly improve interfacial bonding strength and thermal stability.Nano-scratch, micro-scratch, pull-off, and thermal shock tests are employed to systematically evaluate the effects of micro-nano structures on interfacial mechanical performance across different material systems and coating thickness scales.

The results demonstrate that the micro-nano structures markedly enhance interfacial bonding strength and critical

failure load by increasing the effective contact area and introducing pronounced mechanical interlocking effects.In the Cu/SiO_2 system, nanoscale Cu coatings on micro-nano structured substrates remain intact without interfacial delamination under an 80 mN load, while the critical failure load of microscale Cu coatings increases from 6.53 N to 16.62 N, accompanied by a transition from simple interfacial delamination to coupled coating plastic deformation and local structural interlocking.For the Cu/PMMA system, nano-scratch experiments reveal that the micro-nano structures increase the interfacial critical failure load from 5.53 mN to 45.05 mN; however, the enhancement is less pronounced than that observed in the Cu/SiO_2 system.This discrepancy indicates that the interfacial bonding enhancement induced by mechanical interlocking is strongly dependent on the mechanical properties of the substrate material. As PMMA is a relatively soft polymer, its micro-nano structures are more susceptible to plastic deformation or structural collapse under high loads, thereby limiting the effectiveness of mechanical interlocking.At the microscale, although the strengthening effect is constrained by the mechanical properties of the PMMA substrate, the micro-nano structures still improve the pull-off interfacial bonding strength of the Cu/PMMA system by approximately 49 %.Moreover, by extending crack propagation paths and increasing interfacial fracture energy, the micro-nano structures effectively suppress cracking and wrinkling failures in the ITO/PMMA system under thermal shock conditions up to 80 ℃. It should be noted that both single-cycle thermal shock tests and low-cycle thermal cycling experiments have inherent limitations in fully replicating long-term service conditions, and further studies involving extended thermal cycling would be valuable to validate long-term reliability.

This method is primarily suitable for planar substrates or developable surfaces. For non-developable surfaces, achieving uniform and close-packed monolayer microsphere self-assembly is challenging due to variations in curvature and surface tension effects, which can easily lead to mask defects. Meanwhile, the dry etching process requires uniform plasma exposure, which is difficult to maintain on complex curved surfaces, potentially resulting in inconsistent micro-nano structure geometry. Therefore, direct application of this method to workpieces with complex

curved surfaces requires further process optimization to address uniformity issues.

This work provides a simple, low-damage, and broadly applicable route for mechanical reinforcement and thermal reliability improvement of heterogeneous interfaces, offering significant engineering potential for microelectronic packaging, optoelectronic devices, and flexible electronic systems.Future studies may further elucidate the interplay between micro-nano structural geometry and substrate mechanical properties, and extend this strategy to a wider range of material systems and complex service environments.

Author contributions

XXX and XXX: Methodology, Validation, Formal analysis, Writing-original draft. XXX: Investigation. XXX: Data curation. XXX: Supervision. XXX: Supervision, Project administration. XXX: Conceptualization, Funding acquisition.

Acknowledgements

The authors thank the National Natural Science Foundation of China (NSFC) (Grant Nos. 52275200 and 52205312) for financial support.

Declaration of competing interest

The authors have no competing interests to declare that are relevant to the content of this article.

Electronic Supplementary Material

The data for the Nano-scratch tests and the pull-off tests, as well as additional thermal shock experiments on the ITO/PMMA heterogeneous composite materials, are available in the online version

of this article.

References

[1] Yang J, Xiao Q, Lin Z, Li Y, Jia X, Song H. Growth of ultra-dense MoS2 nanosheets on carbon fibers to improve the mechanical and tribological properties of polyimide composites. *Friction*. 2021;9(5):1150-1162. doi:10.1007/s40544-020-0413-0

[2] Kim D, Jeong S, Shin H, Xia Y, Moon J. Heterogeneous Interfacial Properties of Ink-Jet-Printed Silver Nanoparticulate Electrode and Organic Semiconductor. *Advanced Materials*. 2008;20(16):3084-3089. doi:10.1002/adma.200702750

[3] Zhang X, Zhou L, Cai X, et al. Heterogeneous structures and morphological transitions of composite materials and its applications. *Adv Compos Hybrid Mater*. 2024;7(6):251. doi:10.1007/s42114-024-01065-4

[4] Melentiev R, Yudhanto A, Tao R, Vuchkov T, Lubineau G. Metallization of polymers and composites: State-of-the-art approaches. *Materials & Design*. 2022;221:110958. doi:10.1016/j.matdes.2022.110958

[5] Yang C, Wang H, Zhou G, et al. A Multimodal Perception-Enabled Flexible Memristor with Combined Sensing-Storage-Memory Functions for Enhanced Artificial Injury Recognition. *Small*. 2024;20(45):2402588. doi:10.1002/smll.202402588

[6] Aydın EB, Sezgintürk MK. Indium tin oxide (ITO): A promising material in biosensing technology. *TrAC Trends in Analytical Chemistry*. 2017;97:309-315. doi:10.1016/j.trac.2017.09.021

[7] Xu K, Zhou Y, Chen Y, Xie J, Gao Y, Zhu F. Underlying Thinning Mechanisms of Cu/Amorphous SiO_2 Heterostructure in Through Glass Via Wafer from an Atomic Perspective. *J Phys Chem C*.

2025;129(26):12043-12052. doi:10.1021/acs.jpcc.5c00927

[8] Alkhazaili A, Hamasha MM, Choi G, Lu S, Westgate CR. Reliability of thin films: Experimental study on mechanical and thermal behavior of indium tin oxide and poly(3,4-ethylenedioxythiophene). *Microelectronics Reliability*. 2015;55(3-4):538-546. doi:10.1016/j.microrel.2015.01.013

[9] Chawla N, Venkatesh SH, Singh DRP, Alford TL. Characterization and Adhesion in Cu/Ru/SiO2/Si Multilayer Nano-scale Structure for Cu Metallization. *J of Materi Eng and Perform*. 2013;22(4):1085-1090. doi:10.1007/s11665-012-0359-0

[10] Han X, Liu X, Wang D, Wu Z, Duan B. Copper-based tungsten coating by CVD: Microstructure, thermal shock resistance and interfacial bond force. *Surface and Coatings Technology*. 2021;426:127778. doi:10.1016/j.surfcoat.2021.127778

[11] Özbay S. Estimation of the work of adhesion between ITO and polymer substrates: a surface thermodynamics approach. *Turkish Journal of Chemistry*. 2023;47(1):68-80. doi:10.55730/1300-0527.3518

[12] Chen H, Lu BW, Lin Y, Feng X. Interfacial Failure in Flexible Electronic Devices. *IEEE Electron Device Lett*. 2014;35(1):132-134. doi:10.1109/LED.2013.2289932

[13] Hamasha MM, Hamasha S, Alzoubi K, Massadeh R, Hamasha K. Comparative analysis of mechanical and thermal stresses in ITO and AZO thin films on flexible PET substrates for flexible electronic applications. *Microelectronics Reliability*. 2025;175:115921. doi:10.1016/j.microrel.2025.115921

[14] Alzoubi K, Alkhazali AS, Choi G, et al. Comparisons of the Thermal Stability of Poly(3,4-Ethylenedioxythiophene) (PEDOT) and ITO on Flexible Substrates. *IEEE Trans Compon, Packag Manufact Technol*. 2020;10(8):1259-1265. doi:10.1109/TCPMT.2020.3006721

[15] Alanís-Navarro JA, Reyes-Betanzo C, Moreira J, Sebastian PJ. Fabrication and characterization of a micro-fuel cell made of metallized PMMA. *Journal of Power Sources*. 2013;242:1-6. doi:10.1016/j.jpowsour.2013.05.048

[16] Ju H, Ye Y, Feng X, et al. Low-Temperature Growth Improves Metal/Polymer Interfaces: Vapor-Deposited Ca on PMMA. *J Phys Chem C*. 2014;118(12):6352-6358. doi:10.1021/jp500628w

[17] Solodilov V, Kochervinskii V, Osipkov A, et al. Structure and Thermomechanical Properties of Polyvinylidene Fluoride Film with Transparent Indium Tin Oxide Electrodes. *Polymers*. 2023;15(6):1483. doi:10.3390/polym15061483

[18] Hamasha MM, Dhakal T, Alzoubi K, et al. Stability of ITO Thin Film on Flexible Substrate Under Thermal Aging and Thermal Cycling Conditions. *J Display Technol*. 2012;8(7):385-390. doi:10.1109/JDT.2011.2176532

[19] Abhyankar H, Webb DP, West GD, Hutt DA. Characterization of METAL-POLYMER interaction forces by AFM for insert molding applications. *Polymer Engineering & Sci*. 2020;60(12):3036-3045. doi:10.1002/pen.25534

[20] Yudhanto A, Li X, Tao R, Melentiev R, Lubineau G. Identifying adhesion characteristics of metal-polymer interfaces: Recent advances in the case of electroplated acrylonitrile butadiene styrene. *Materials Today Communications*. 2023;35:106218. doi:10.1016/j.mtcomm.2023.106218

[21] Liu J, Xue Y, Dong X, Fan Y, Hao H, Wang X. Review of the surface treatment process for the adhesive matrix of composite materials. *International Journal of Adhesion and Adhesives*. 2023;126:103446. doi:10.1016/j.ijadhadh.2023.103446

[22] Alsheghri AA, Alageel O, Amine Mezour M, et al. Bio-inspired and optimized interlocking features for strengthening metal/polymer interfaces in additively manufactured prostheses. *Acta*

Biomaterialia. 2018;80:425-434. doi:10.1016/j.actbio.2018.09.029

[23] Nsilani Kouediatouka A, Ma Q, Liu Q, Mawignon FJ, Rafique F, Dong G. Design Methodology and Application of Surface Texture: A Review. *Coatings*. 2022;12(7):1015. doi:10.3390/coatings12071015

[24] Xu Y, Qiu X, Wang S, Su J, Xing F, Wang H. High temperature thermo-mechanical responses mediated by interfacial microstructure regulation in tungsten heavy alloy/superalloy brazed joints. *Journal of Materials Research and Technology*. 2023;24:2688-2702. doi:10.1016/j.jmrt.2023.03.190

[25] Cao X, Li M, Zhang L, et al. Improvements of the interfacial adhesion between water-based coating and carbon fiber reinforced polymer composite by deposition of silica particles. *J Sol-Gel Sci Technol*. 2023;108(3):878-888. doi:10.1007/s10971-023-06226-3

[26] Yu S, Wang Y, Wang S, et al. Inspired square micro-texture structures designed by nanosecond laser sculpture for enhancing adhesion strength of plasma spraying Si-HfO2 bond coat on SiC substrates. *Optics & Laser Technology*. 2024;175:110840. doi:10.1016/j.optlastec.2024.110840

[27] Hsissou R, Seghiri R, Benzekri Z, Hilali M, Rafik M, Elharfi A. Polymer composite materials: A comprehensive review. *Composite Structures*. 2021;262:113640. doi:10.1016/j.compstruct.2021.113640

[28] Nagao K, Neaton JB, Ashcroft NW. First-principles study of adhesion at C u / S i O 2 interfaces. *Phys Rev B*. 2003;68(12):125403. doi:10.1103/PhysRevB.68.125403

[29] Lozano JG, Lozano-Perez S, Bogan J, et al. Interdiffusion and barrier layer formation in thermally evaporated Mn/Cu heterostructures on SiO2 substrates. *Applied Physics Letters*. 2011;98(12):123112. doi:10.1063/1.3569146

[30] Zhou B, Randall N, Prorok B. Correlation between Adhesion Strength and Thin film/Substrate

Mechanical Properties using the Nano-Scratch Technique. *MRS Proc*. 2011;1297:mrsf10-1297-p03-07. doi:10.1557/opl.2011.651

[31] Gasparin AL, Wanke CH, Nunes RCR, et al. An experimental method for the determination of metal–polymer adhesion. *Thin Solid Films*. 2013;534:356-362. doi:10.1016/j.tsf.2013.03.018

[32] Yang B, Chen G.Mechanics of Coatings and Thin Films. Beijing: Beijing Institute of Technology Press Co.2020.

[33] Feng B. Tribology behavior on scratch tests: Effects of yield strength. *Friction*. 2017;5(1):108-114. doi:10.1007/s40544-017-0148-8

[34] Zhou X, Zhu Y, Yang C. Nanosurface Engineering and Mechanics. Beijing: China Machine Press,2012.

[35] Li Z, Yang M, Qian H, et al. Modern Surface Engineering Technologies. Beijing: China Machine Press, 2007.

[36] Er GS, Yhaya MF, Teik PB. Characterisation and adhesion properties of UV-cured natural rubber-based adhesives. *International Journal of Adhesion and Adhesives*. 2023;123:103347. doi:10.1016/j.ijadhadh.2023.103347

[37] Han JC, Wang BL. Thermal shock resistance enhancement of functionally graded materials by multiple cracking. *Acta Materialia*. 2006;54(4):963-973. doi:10.1016/j.actamat.2005.10.036

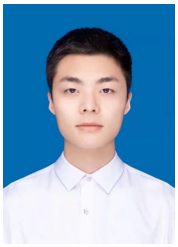

Zeyu Wang. He received his B.E. degree in Mechanical Engineering from the School of Mechanical

Engineering, Anhui University of Technology, China, in 2023. He is currently a master's student at the School of Mechanical and Electrical Engineering, Beijing University of Civil Engineering and Architecture, China. His research interests focus on micro- and nano-manufacturing.

Yiming Li. He received his Bachelor of Engineering degree from the Department of Mechanical Engineering, Tsinghua University, China, in 2024. He is currently a Ph.D. candidate in the Department of Mechanical Engineering at Tsinghua University. His research interests focus on the fabrication of interfacial micro/nano structures.

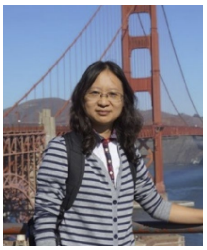

Hua Qin. She received her Ph.D. degree from Tsinghua University, China, in 2009. She is currently a professor at the School of Mechanical and Vehicular Engineering, Beijing University of Civil Engineering and Architecture, China, Her research interests include micro- and nano-manufacturing.

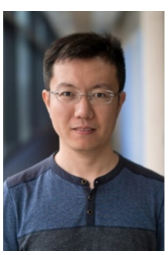

Yan Ma. He received his Ph.D. degree from the University of Chinese Academy of Sciences, China, in 2017. He is currently an assistant research fellow at the Department of Mechanical Engineering, Tsinghua University, China. He was a jointly trained Ph.D. student and postdoctoral researcher at Weill Cornell Medicine and the Houston Methodist Research Institute from 2015 to 2018, and a postdoctoral researcher at the Leslie Dan Faculty of Pharmacy, University of Toronto, Canada, from 2018 to 2020. His research interests include microfluidic technologies and interfacial regulation.

Jiadao Wang. He received his Ph.D. degree from the Department of Precision Instruments, Tsinghua University, China, in 2000. He is currently a tenured professor at Tsinghua University, serving as the Head of the Department of Mechanical Engineering and the Director of the Tsinghua Tianjin Institute of Advanced Equipment. He previously served as the Dean of the School of Mechanical Engineering, Tsinghua University, from 2023 to 2025. His research interests focus on interfacial effects and their control, including surface drag reduction, wetting behaviors such as superhydrophobicity, and colloidal self-assembly.